J Membrane Biol (2013) 246:495–511
DOI 10.1007/s00232-013-9564-5

Implications of Aberrant Temperature-Sensitive Glucose Transport Via the Glucose Transporter Deficiency Mutant (GLUT1DS) T295M for the Alternate-Access and Fixed-Site Transport Models

Philip Cunningham · Richard J. Naftalin

Received: 20 December 2012 / Accepted: 15 May 2013 / Published online: 6 June 2013

Abstract In silico glucose docking to the transporter GLUT1 templated to the crystal structure of *Escherichia coli* XylE, a bacterial homolog of GLUT1–4 (4GBZ.pdb), reveals multiple docking sites. One site in the external vestibule in the exofacial linker between TM7 and -8 is adjacent to a missense T295M and a 4-mer insertion mutation. Glucose docking to the adjacent site is occluded in these mutants. These mutants cause an atypical form of glucose transport deficiency syndrome (GLUT1DS), where transport into the brain is deficient, although unusually transport into erythrocytes at 4 °C appears normal. A model in which glucose traverses the transporter via a network of saturable fixed sites simulates the temperature sensitivity of normal and mutant glucose influx and the mutation-dependent alterations of influx and efflux asymmetry when expressed in *Xenopus* oocytes at 37 °C. The explanation for the temperature sensitivity is that at 4 °C glucose influx between the external and internal vestibules is slow and causes glucose to accumulate in the external vestibule. This retards net glucose uptake from the external solution via two parallel sites into the external vestibule, consequently masking any transport defect at either one of these sites. At 37 °C glucose transit between the external and internal vestibules is rapid, with no significant glucose buildup in the external vestibule, and thereby unmasks any transport defect at one of the parallel input sites. Monitoring glucose transport in patients' erythrocytes at higher temperatures may improve the diagnostic accuracy of the functional test of GLUT1DS.

Keywords Glucose transport · GLUT1 glucose transporter deficiency · Mutation · Simulation

P. Cunningham
Bioinformatics Division, School of Medicine, King's College London, Franklin–Wilkins Building, Waterloo Campus, London SE1 9HN, UK

R. J. Naftalin (✉)
Cardiovascular and Physiology Division, School of Medicine, King's College London, Franklin–Wilkins Building, Waterloo Campus, London SE1 9HN, UK
e-mail: richard.naftalin@kcl.ac.uk

Introduction

Glucose transporter (GLUT1) deficiency syndrome (GLUT1DS) impacts on medicine and biology. The syndrome is caused by diminished glucose transport across the blood–brain barrier, resulting from a dysfunction of the passive facilitative glucose transporter (GLUT1, SLC2A1). This is manifest as a low glucose concentration in the cerebrospinal fluid, <2.2 mM, termed "hypoglycorrhachia" (Rotstein et al. 2010). Infants with the syndrome have intractable epileptic encephalopathy, associated with movement disorders that may be exacerbated by exercise or fasting. The disease results in retarded neurological development and may lead to acquired microcephali and mental retardation.

Diagnosis is based on finding hypoglycorrhachia in the absence of encephalitis or hypoglycemia, together with the presence of a mutation in the *SLC2A1* gene (Klepper 2012), and is corroborated by observing decreased uptake of 3-*O*-methyl-D-glucose (3OMG) into the patient's own erythrocytes, ≈50 % of control rate, and by observing mutations in the mRNA sequence of GLUT1.

To date, over 500 cases have been identified worldwide. The GLUT1DS phenotype varies widely in severity; the extent of neurological dysfunction correlates with the extent of hypoglycorrhachia (Brockmann 2009). Early

diagnosis of the condition is very important as treatment with a ketogenic diet can ameliorate the effects of the disease, particularly with regard to epileptic seizure frequency, by providing the brain with short-chain fatty acids as an alternative energy source to glucose (Rotstein et al. 2010).

Diagnosis of GLUT1DS depends on accurate assessment of the clinical and biochemical signs. However, in some cases measurement of the rate of uptake of 3OMG into the patient's erythrocytes leads to an erroneous diagnostic conclusion (Fujii et al. 2011; Wang et al. 2003, 2008; Wong et al. 2007).

With the single-substitution T295M missense mutant, although the clinical phenotype does not differ from that of other GLUT1DS patients, particularly with respect to hypoglycorrhachia and seizure frequency, the maximal rate of erythrocyte uptake of 3OMG is not significantly decreased compared with controls. These findings contrast with earlier reports, where 2-deoxy-D-glucose (2-DG) was used to monitor uptake in CHO-KI cells after expression of the transfected control GLUT1 or the GLUT1 mutant T295M DNA. The missense T295M mutant had a V_{max} for 2-DG uptake around 50 % of control—no different from six other missense mutants (Tables 1, 2). In *Xenopus* oocytes expressing T295M GLUT1 a 30 % reduction in 3OMG influx and an 80 % inhibition of the maximal rate of 3OMG efflux were observed (Fujii et al. 2011; Wang et al. 2003, 2008; Wong et al. 2007).

Since the extent of hypoglycorrhachia and the neurological dysfunction in T295M GLUT1DS patients are similar to those of others with missense mutants, this might suggest a differential selectivity between 3OMG and 2-DG for influx via GLUT1. This view can now be dismissed because influx of both 2-DG and 3OMG into erythrocytes with the missense mutant T295M is similar to control influx (D. C. De Vivo, personal communication, 2012).

Table 1 Analysis of 3OMG kinetics of wild type (WT) and T295M mutant in *Xenopus* oocytes

Condition	Parameter	WT	T295M	WT/T295M
Influx	$K_{m\ out}$ (mM)	9.6	14.3	0.7
	$V_{max\ out}$ (pmol/min/oocyte)	747.0	590.0	1.3
	V_{max}/K_m	77.8	41.3	1.9
Efflux	$K_{m\ in}$	90.8	8.8	10.3
	$V_{max\ in}$ (pmol/min/oocyte)	7,443.0	1,216.0	6.1
	$V_{max\ in}/K_{m\ in}$	82.0	138.2	0.6
Asymmetry	$K_{m\ in}/K_{m\ out}$	9.5	0.6	15.8
	$V_{max\ in}/V_{max\ out}$	10.0	2.1	4.8
	Haldane ratio	1.1	3.3	0.3
	$V_{max\ in}/K_{m\ in}/(V_{max\ out}/K_{m\ out})$			

Data from Wang et al. (2003)

Table 2 Analysis of 2-DG influx kinetics WT and T295M in CHO cells

Condition	Parameter	WT	T295M
Influx	$K_{m\ out}$ (mM)	2.7	2.9
	$V_{max\ out}$ (pmol/min/mg protein)	23.4	12.2
	V_{max}/K_m	8.6	4.2

Data from Wong et al. (2007)

A suggested explanation for the paradoxically normal influx associated with a positive GLUT1DS hypoglycorrhachia phenotype is that the sugar fails to exit from the brain capillary endothelial cells into the brain interstitial fluid (Klepper 2012). It is assumed that net glucose exit is retarded at the GLUT1DS export sites situated on the endothelial basal membrane, which has a low V_{max} and K_m for the sugar. However, this fails to account for the decreased V_{max} for 2-DG influx reported when the T295M mutant is expressed in CHO cells (Fung et al. 2011; Wong et al. 2007) (Tables 1, 2).

Another GLUT1 mutation caused by a four–amino acid insertion between residues 298 and 299 (glutamine, glutamine, leucine serine, QQLS) in the exofacial linker between TMs 7 and 8 has similar characteristics to the T295M—namely, absence of inhibition of 3OMG influx into erythrocytes—yet this patient too had hypoglycorrhachia and epilepsy that responded positively to a ketogenic diet (Fujii et al. 2011).

An interesting aspect of the reported 3OMG transport data is the large difference in the symmetry of the wild-type transport system compared with the T295M mutant (Wong et al. 2007). The ratio of K_m values of 3OMG for efflux and influx in wild-type GLUT1 is ~5–10. The ratio of V_{max} for efflux and influx is similarly asymmetric, giving a Haldane ratio—i.e., $(V_m/K_{m\ efflux})/(V_m/K_{m\ influx})$—of ~1.0 (Table 1). Although these flux parameters are consistent with a passive alternating single-site carrier (Lieb and Stein 1974), the model requires that the rates of vacant carrier movement be asymmetric. This can only be attained by the implicit assumption that these asymmetric rates are generated by an exogenous energy source (Naftalin 2008, 2010). The T295M GLUT1 mutant alters the ratio of K_m values of 3OMG net efflux and influx to ≈0.6 and the V_{max} ratio to 2.1. Both ratios are smaller than with control GLUT1. Thus, T295M mutation alters the asymmetry of the transporter for 3OMG transport from a tenfold lower affinity ratio in control cells to a nearly twofold higher affinity ratio at the inner site. The mutation also causes a 21 % reduction in V_{max} for net entry but an 83 % reduction in V_{max} for net exit and raises the Haldane ratio of the mutant T295M transport system to 3.3.

A major difference between the protocols used for observing glucose influx in the patients' erythrocytes is that the temperature used to measure sugar influx into erythrocytes is usually 4 °C, whereas the fluxes in CHO cells or oocytes are measured at 37 °C. The low temperature is used to measure flux in erythrocytes because at 37 °C equilibration of 3OMG is complete within a few seconds and, thus, is unsuited for measurement of radiolabeled sugar uptake. CHO cells and oocytes have three and six orders larger volume, respectively, than erythrocyte volume, 90 fl, and relatively fewer GLUTs expressed within their plasma membranes; consequently, glucose equilibration takes longer in these cells and, thus, can be readily monitored at 37 °C.

However, this temperature difference, besides altering flux, may also result in a qualitative change in kinetics. Thermosensitive transport mutations have been described where the mutant phenotype is observed only at raised temperature but at lower temperatures is apparently "stable," as seen with CFTR (Liu et al. 2012) and thermosensitive mutants of the uric acid/xanthine $Uapa^{+}$ transporter in *Aspergillus nidulans* (Pantazopoulou and Diallinas 2006).

We have previously used a 3D template structure for GLUT1, as generated by Salas-Burgos et al. (2004) to dock glucose derivatives and inhibitors of glucose transport (Cunningham et al. 2006). Recently, a crystal structure of an *Escherichia coli* homolog, XylE, of the glucose transporters GLUT1–4 has been described (Sun et al. 2012). We used this crystal structure as a revised template of GLUT1. The templates generated by both Swiss-Model (http://swissmodel.expasy.org/), a fully automated homology-modeling server, and another similar program, I-Tasser Online (http://zhanglab.ccmb.med.umich.edu/I-TASSER), are virtually identical and similar to the GLUT1 template generated by Sun et al. (2012).

Here, a recently revised version of the molecular docking program Autodock, Autodock Vina (http://vina.scripps.edu/download.html), was used to find the possible docking positions of glucose and other transported ligands on GLUT1 and GLUT1 mutants. Autodock Vina improves the precision and docking speeds by at least two orders of magnitude, completing docking searches in minutes where previously many hours were required. However, it uses a quasi-Newtonian optimization method where a scoring function and its gradient are used to reach an equilibrium docking position, differing from the quasi-Lamarckian algorithm used in the previous versions of Autodock. The new scoring function is a weighted approximation of the standard chemical potentials of the van der Waals and coulombic interactions of the system (Seeliger et al. 2011; Seeliger and de Groot 2010). We have found that Autodock Vina gives almost identical docking patterns to those obtained with Autodock III for glucose docking on the GLUT1 template we used previously (Cunningham et al. 2006).

We used the new templates for GLUT1 and the T295M mutation and insertion mutation QQLS between GLUT1 298 and 299 (Fujii et al. 2007) to dock glucose and other hexose analogs to determine if the mutations alter the docking pattern in ways which are consistent with the altered transport activity. Additional computational resources included Open Babel: The Open Source Chemistry Toolbox (http://openbabel.org/) and hand-crafted Perl scripts run on Sun Microsystems SunOS 5.9. Structures were viewed in Jmol (http://jmol.sourceforge.net/), an open-source Java viewer for chemical structure, and Swiss_pdbViewer 4.1.0 (http://spdbv.vital-it.ch/).

An alternative transport model with some similarities to totally asymmetric exclusion processes (Chou et al. 2011; Parmeggiani et al. 2004) has been used here to simulate the sugar fluxes in control and mutant transporters. In this model it is assumed that transported ligands diffuse between adjacent nodes via an intermediate space in a network of sites traversing the transporter. This model simulates all the kinetic phenomena observed with the T295M mutant to date.

Methods

Molecular Docking of Sugar Ligands to GLUT1

The 3D data files were collected from the following sources: GLUT1 (1SUK) and the crystal structure of a bacterial glucose transporter, 4GBZ.pdb, obtained from the public domain Protein Data Bank in Europe (http://www.ebi.ac.uk/pdbe/).

Modeling of the GLUT1 template displayed here was performed with Swiss-Model, using the automated mode requesting that sequence data be aligned to the 3D template 4GBZ.pdb (obtained from http://www.ebi.ac.uk/pdbe/). Molecular displays were created by Swiss-PdbViewer (http://spdbv.vital-it.ch/) 4.1.0 and RasMol (openrasmol.org/). The 3D structures of the sugar ligands were generated and corroborated within Chemsketch (http://www.acdlabs.com/resources/), and PDB files were transferred to Vina. A rectangular parallelepiped, aligned with the protein coordinate system, was drawn around the selected search position; the search space in any dimension had a minimal value of 22.5 Å. The default settings of Vina (Trott and Olson 2010) were normally used. Docking of D-glucose, 2-DG and 3OMG using Vina on the template 3D structure of GLUT1 and the mutant GLUT1 T295M were compared with dockings obtained previously using Autodock III. In silico mutation of GLUT1 to the GLUT1DS mutant T295M and other amino acids was performed using the mutate tool facility in Swiss-Prot Deepview. The various rotamer forms of Met-295 were generated using the torsion tool in Swiss-Prot Deepview, and then the

PDB file was subjected to energy minimization using the Groningen machine for chemical simulation (GROMACS) algorithm within Deepview. The probity and angular conformations of these methionine rotamers generated in silico were corroborated using the online program Molprobity (http://molprobity.biochem.duke.edu/).

The QQLS Insertion Between Residues 298 and 299 in GLUT1

As mentioned above, a 4-mer insertion mutation between positions 298 and 299 develops similar kinetic characteristics to those of T295M (Fujii et al. 2007). We investigated whether this GLUT1 mutation has similar docking characteristics to those of T295M. The QQLS insertion was generated by using the automatic modeling mode of SwissProt Deepview in the template version of GLUT1 4GBZ.pdb (Sun et al. 2012) and followed by reequilibration of the protein construct with GROMACS (see below, Fig. 3).

Simulation of Glucose Transport Using a Multisite Model

A multisite kinetic model of the GLUT1 transporter was generated using Berkeley Madonna (version 8.3.18, http://www.berkeleymadonna.com/). This multisite model is an extension of a two-site model described previously (Carruthers et al. 2009; Naftalin 2010). Two sites in the external vestibule provide a parallel feed from the external solution to a third high-affinity central site lying within the depths of the external vestibule and in series with sites 1 and 2. This central site is connected serially to a fourth low-affinity site lying within the inner vestibule. This inner site has access to the internal solution (Figs. 5, 6).

Transported sugars are assumed to accumulate within a low volume space lying between all three sites in the external vestibule. When glucose concentrations on either side of the transport are equal, ligand equilibration occurs within the intersite space to the same concentrations as present in the external solutions. The model configuration permits variable ligand selectivity at the external face of GLUT1 as deletion of one or the other external sugar binding site may alter the net resultant selectivity if the affinities at sites 1 and 2 differ.

Results

Docking of D-Glucose on the GLUT1 Template and the T295M Missense Mutation

The template of GLUT1 on the crystal structure of its bacterial homolog was used to dock glucose and glucose derivatives, i.e., 2-DG and 3OMG. Thr-295 is positioned in GLUT1 in the external linker region between transmembrane helices 7 and 8 (Mueckler et al. 1985; Salas-Burgos et al. 2004). In the 3D template of the GLUT1 structure this is situated in the rim of the outer vestibule (Fig. 1). In addition to the centrally placed high-affinity docking site for glucose, reported by Sun et al. (2012), lying midway between the external and internal vestibules in a confined position, several lower-affinity sites are evident in both the external and internal vestibules. In the external vestibule three lower-affinity docking sites lie within a radial distance of 5 Å of Thr-295 in the linker between TMs 7 and 8. As estimated by Autodock Vina the K_i values of glucose at these docking sites vary from 250 to 500 μM, whereas the highest-affinity docking site has an estimated K_i of 5 ± 1.5 μM. The distance between Thr-295 and any of these docked sugar residues is too large to form any H-bonding interaction. Another two clusters lie between TMs 1, 5 and 7b in the external vestibule. The more external cluster has a higher estimated K_i, 310 μM, than the more centrally sited cluster, 50 ± 15 μM.

In addition there are four clusters docking in the inner vestibule. Three of these lie close to the helical regions within the cytoplasmic linker region between TMs 6 and 7. This helical region has been revealed by the new crystallographic data (Sun et al. 2012). A fourth cluster is more isolated from the others. All four clusters have affinities ranging between 160 and 270 μM. Their main characteristic is that all lie at entrance sites to the vestibular cage region surrounded by the C-terminal region, the linker between TMs 6 and 7 and the cytoplasmic region of TM 11.

Mutating T295 to M295 results in occlusion of one of the low-affinity glucose docking sites (Fig. 2). There are 27 preferred rotamer conformations of methionine (Butterfoss and Hermans 2003). Several Met-295 rotamer conformations either prevent or differentially curtail D-glucose, 2-DG or 3OMG docking, indicating that due to a reduced size of the docking cavity the number of possible hexose docking positions is curtailed.

Similarly, insertion of the 4-mer peptide between positions 298 and 299 lengthens the TM 7b loop and results in occlusion of the same glucose docking site as is affected by M295 missense mutation (Fig. 3a–c).

Although it is evident that the larger bulk of the methionyl side chain at M295 than with T295 or the 4-mer insertion between 298 and 299 can directly occlude the adjacent glucose binding site, it is also likely that these mutations block one of the available pathways for glucose diffusion between the external solution and the high-affinity central binding site. In the control GLUT1 transporter it appears that two grooves on the external vestibular

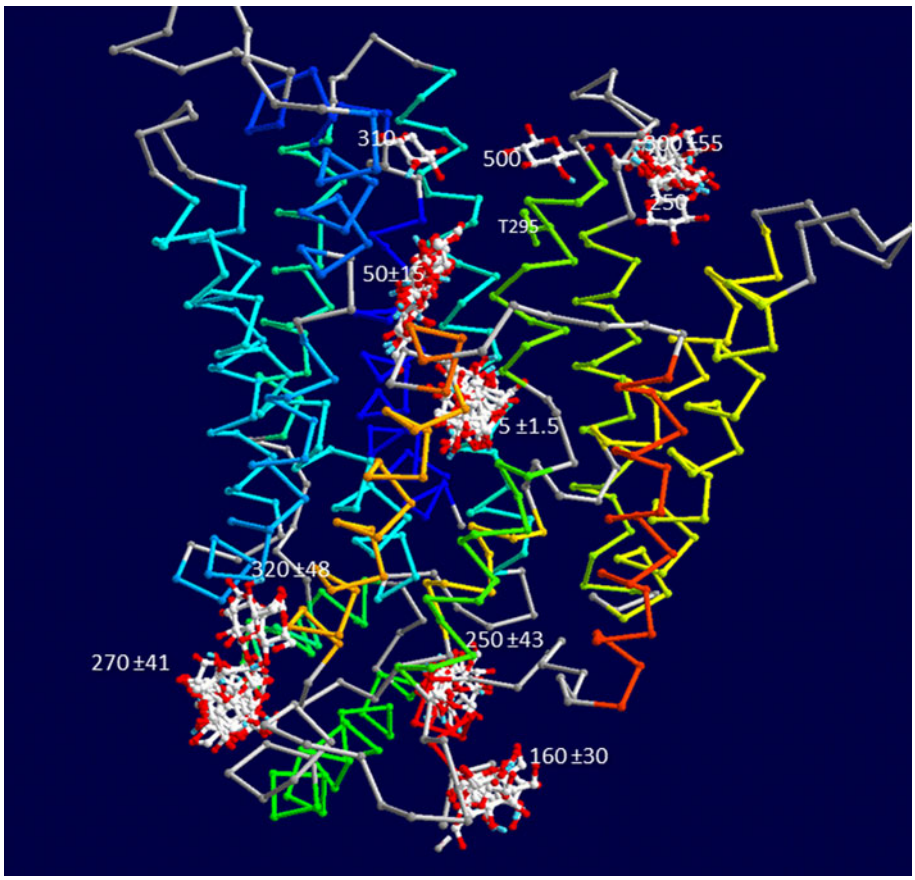

Fig. 1 The docking clusters obtained by docking D-glucose onto a template version of GLUT1 with Autodock Vina. The figure was obtained by superimposing 10 dockings, each localized within parallelepipeds arranged to give overlapping high-resolution searches over the entire protein structure. The nine ligands with highest affinities are reported for each docking search, so some clusters which appear in two or more overlapping searches are more heavily populated. The affinities (μM ± SEM) are obtained from estimates of energy of interaction as obtained by Autodock Vina (Trott and Olson 2010). The color coding of the TM segments is from N- to C-terminal 1–12. As reported by Sun et al. (2012), the internally facing linker region between TMs 6 and 7 has two alpha-helical segments which have been unremarked previously. It is evident that the central site has a much higher affinity than all the others, thereby generating a nuclear attraction drawing glucose toward the center of the transporter from either the external or the internal bathing solution

surface connect binding sites 1 and 2 at the external surface with the central binding glucose docking to the central docking site shown in Fig. 4. One groove is between TMs 5 and 6 and the other, between TMs 7b and 8. This latter may be subject to blockage by the mutations at T295 or the 4-mer insertion between F298 and E299.

Figure 3d shows the docking poses of several other mutations, GLUT1 295. Substitution of serine cysteine for threonine permits docking patterns that are similar to those in control with threonine at position 295. Alanine substitution of T295, as with some of the methionine rotamers, prevents docking at the site closest to position 295. Surprisingly, we observed that T295V permits docking at the adjacent site, albeit with a lower affinity than threonine. These findings may suggest that amino acids with hydrophilic side chains are acceptable substitutions for threonine. However, glycine and alanine give aberrant results: glycine substitution permits glucose docking but with a fivefold higher affinity than threonine, whereas alanine substitution prevents docking at the adjacent site.

A Model for Differential Asymmetric Influx and Efflux of 3OMG and 2-DG

Docking studies (Cunningham et al. 2006; Salas-Burgos et al. 2004) and mutation studies with various GLUT isoforms, particularly involving GLUT7, have suggested that selectivity motifs for various hexoses are present in the linker regions at the external face of the transporter (Manolescu et al. 2005, 2007). Selectivity sites in the peripheral exofacial zone cannot simultaneously serve as an exo-endofacial inversion site.

The alternating-access model of glucose transport requires that the binding site be exposed either to the outside extracellular or inside cytosolic solution. Central placement of the binding site is necessary to minimize the

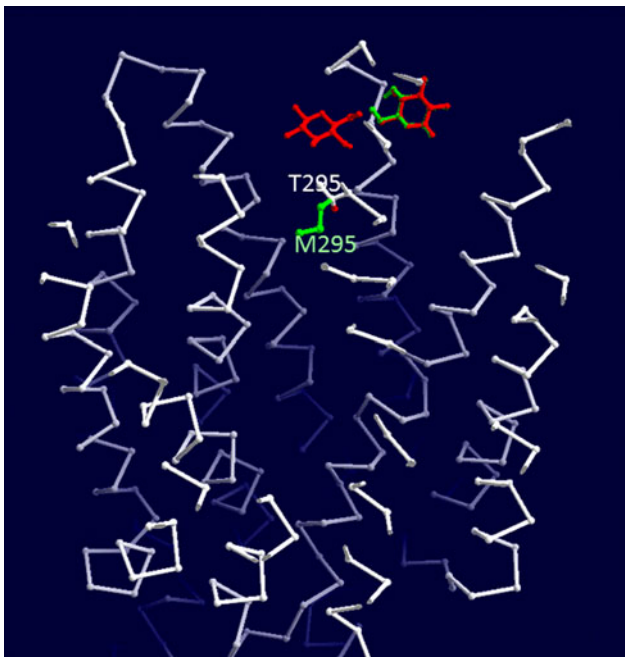

Fig. 2 Slab view, 20 Å thick, centered on the external vestibule of GLUT1 templated to *E. coli* XylE 4GBZ.pdb showing superimposed dockings of two D-glucose sites close to T295 in the external vestibule (*red*) and a rotamer of M295 that occludes glucose docking to one vestibular site (*green*) (Color figure online)

energy required for inversion between outside and inside facing conformations.

The presumed central location of the single binding site is the basis of several studies involving chimeric forms of GLUT1 and -2 (Seatter et al. 1998). Thus, from structural and kinetic viewpoints, any mutation in an external facing loop that greatly increases the affinity of the inward facing site and reduces the maximal rate of zero-trans net exit of glucose defies explanation by the alternating-access model.

Transformation of Wild Type to T295M Hexose Transport Kinetics

A more plausible explanation for the critical role of the M295T mutant in altered asymmetry of the glucose transporter is to regard ligand transport via GLUT1 as the result of a random walk of the transported sugar between the two sides of the transporter along the length of the central hydrophilic channel between sites of varying affinity. The mutation is assumed to alter the ligand diffusion rate and trajectory mainly in its vicinity. However, alterations in trajectory within a branched network can have unexpected consequences at more distant locations. A simple two-site model describing the observed asymmetric hexose transport across GLUT1 and the apparent multiphasic rates of glucose equilibration into human erythrocytes has been discussed previously (Carruthers et al. 2009; Naftalin 2008, 2010). However, an explanation for the observed differences in kinetics between wild type and T295M requires a more complex network with a minimum of three to four binding sites. Sites 1 and 2 within the external vestibule face outward to the external solution and are connected with the central site 3 and to each other via the intersite space within the external vestibule. Site 3 is also connected to site 4 in the inner vestibule via another intersite space lying within the narrow central channel, which connects the external and internal vestibules. The intersite spaces between sites 1, 2 and 3 and between sites 3 and 4 are occluded from both external and cytosolic solutions. Sugar can only enter these spaces via the adjacent sites (Fig. 5).

This minimal model assumes that substitution of methionine for threonine at position 295 or insertion of amino acids between F298 and E299 slows the rates of hexose association and dissociation to and from site 1 (Figs. 4, 6, 7, 8, 9, 10, 11, 12). These assumptions permit simulations in good quantitative agreement with those observed with the T295M GLUT1DS mutant for both 2-DG and 3OMG (Wang et al. 2003, 2008; Wong et al. 2007) (Figs. 9, 10).

Decreased 2-DG Influx

Decreased 2-DG influx at 37 °C in the T295M GLUT1DS mutant is readily explained by the multisite model (Figs. 7, 8). In control GLUT1, parallel access to the central site 3 is via sites 1 and 2 and the intermediate intersite space within the external vestibule. Sites 1 and 2 for 2-DG uptake into the wild-type GLUT1 have assigned affinities of 0.2 and 0.1 mM, respectively, and rates of association of 100 s^{-1} at 37 °C. Sites 3 and 4 have affinities for 2-DG of 10 and 1 mM, respectively. The mutation T295M is assumed to slow rates of both association and dissociation to 1 s^{-1} at site 1, allowing the affinity to remain unchanged at 0.2 mM. Association and dissociation rates to site 2 are unaltered. The resultant net flow is a reduced net maximal rate of zero-trans net influx across the transporter by ~60 % without any substantial alteration of the K_m. However, maximal flow through site 1 is reduced by approximately 98 %. Simulation of 2-DG influx with these parameters is in agreement with experimental observations (Wong et al. 2007). The relatively slow sugar permeability of the path connecting sites 3 and 4 leads to sugar accumulation within the external vestibule. This buildup in vestibular sugar accumulation retards net influx via both sites 1 and 2. However, blockage at site 1 reduces vestibular sugar accumulation, and this results in a compensatory increase in sugar flow via site 2. Because influx via site 2 is raised by 50 %, the V_{max} of net flow across the transporter network is reduced by only 60 % (Fig. 8b, c).

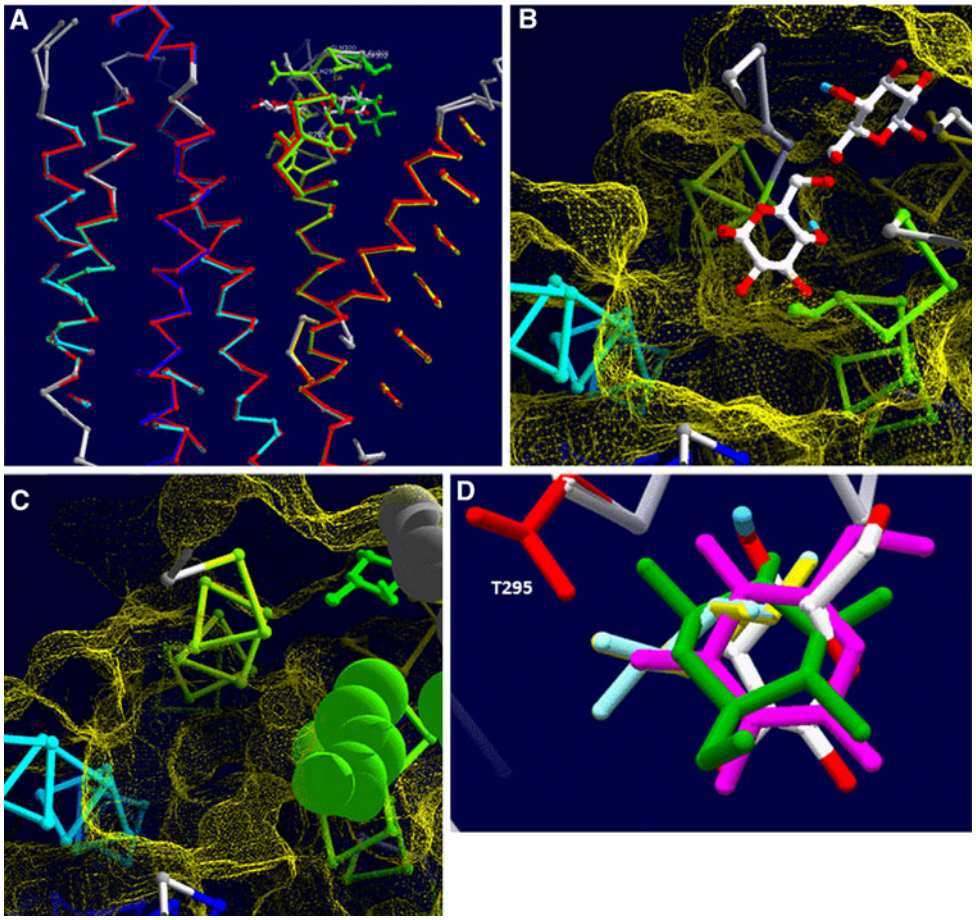

Fig. 3 **a** Superimposed templates of GLUT1 view from in front, in which the TMs are colored by order 1–12 (*blue* to *red*) and GLUT1 with a QQLS 4-mer insertion between F298 and E299 (Fujii et al. 2011) obtained as described in "Methods section" (*green*). The positions of glucose docking for control are shown in CPK colors and for the 4-mer insert in *green*. Note the absence of glucose docking at the more centrally positioned glucose docking site. **b** Slab view of glucose docking to the control GLUT1 template as shown in **a** and viewed from above. The *yellow mesh* is the molecular surface as drawn by Swiss-pdb Viewer 4.1.0. **c** Similar view to that shown in **b** except the docking is to the template version of the QQLS insertion between F298 and E299 side chains shown as *green spheres*. In contrast with control, no glucose is docked in the foreground. **d** Docking of D-glucose to GLUT1 glucose site 1 with various mutations at position 295. The *red* side chain shows the position of T295. There was no docking with A295 or M295 rotamer 5 at site 1. The glucose ligand in CPK shows glucose docking at T295. The highest affinity of the ligands docked with other amino acid substitutions at 295 is shown as follows (K_i, mM): T295 CPK 4.6, T295C *yellow* 1.28, T295S *cyan* 1.28, T295G *green* 0.8, T295V *violet* 6.4 (Color figure online)

Simulation of Zero-trans Net Glucose, 2-DG or 3OMG Influx at 4 °C

The maximal rate of glucose influx into human erythrocytes is slowed by nearly 100-fold by temperature reduction from 20 to 0 °C (Sen and Widdas 1962; Brahm 1983; Lowe and Walmsley 1986; Whitesell et al. 1989). Glucose net influx exceeds net efflux by more than threefold; hence, flux asymmetry is enhanced as temperature is reduced. This is explained in terms of the single alternating-site model by postulating that return of the vacant carrier from inside to outside has a higher activation energy than any of the other rates of loaded or vacant carrier flux. Net hexose influx of 3OMG (Fujii et al. 2007) or 2-DG (D. C. De Vivo, personal communication) into the T295M mutation does not differ from control. The only explanation for this that the alternating-access model can offer is that the mutant does not alter transport at this temperature. Thus, T295M can be considered to be a thermosensitive mutant.

The absence of any observable decrease in either 2-DG or 3OMG influx at 4 °C can now be explained as due to the temperature-sensitive slowing of sugar transit between the external and internal vestibules because of a reduced dissociation rate from site 3 and slower diffusion through the narrow central channel to site 4 (Fig. 8d–f). This results in a much higher sugar accumulation into the external vestibule at any external sugar concentration (Fig. 8c, f). Hence, sugar entry from the external solution via both sites 1 and 2

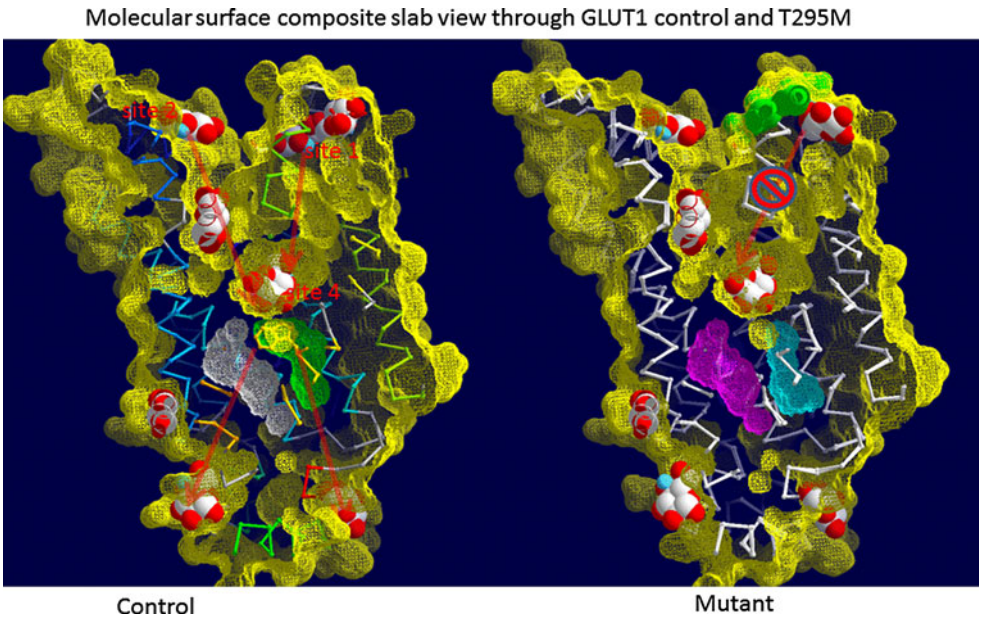

Fig. 4 The putative pathways between docking sites 1 and 4 and sites 2, 3 and 4. *Left* The external vestibule has two delineated pathways which could be routes for glucose diffusion between external sites 1 and 2 and the central high affinity site 4

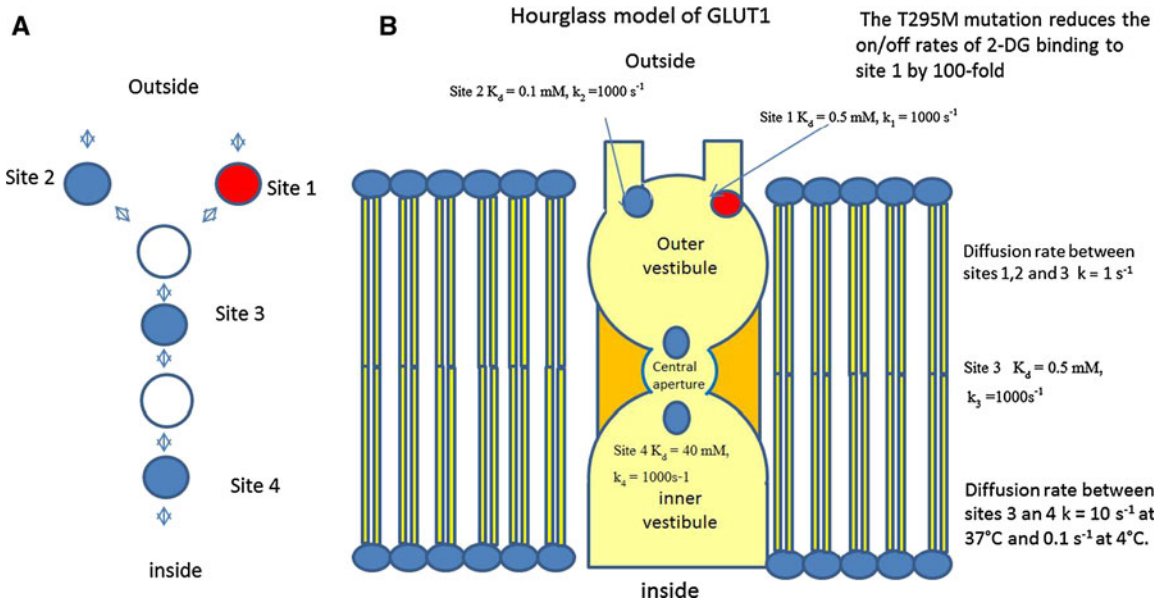

Fig. 5 Diagram showing the hourglass model of the transport network of sites connecting the clusters in the outer vestibule with the central and inner part of GLUT1. **a** Model of network of sites and intersite spaces across the network. Sites 1 (*red*) and 2 correspond to the two external sites in the outer vestibule; both are connected to the external solution and to site 3 via an intermediate space. Site 4 is connected to site 3 via an intermediate space and to the cytosolic solution. The approximate positions of the sites within GLUT1 are shown in **b** diagrammatically, the position of T295M. It is proposed that the mutation T295 and the QQLS insertion between 298 and 299 greatly retard ligand association and dissociation rates to site 1 and, hence, reduce net influx and efflux via this site (Color figure online)

is retarded. The reduced glucose permeability via mutated site 1 reduces sugar accumulation into the external vestibule, but this results in a compensatory increase in sugar uptake via the unaffected site 2 by more than 200 % (Fig. 8e). The higher rate of uptake via site 2 entirely masks the retarded sugar flux via the mutated site 1 as net flux is unaltered (Fig. 8d). Thus, at 4 °C no change in sugar influx is detectable between control and mutant GLUT1.

Asymmetric Effects of T295M Mutation on 3OMG Fluxes

Modeling 3OMG net influx and efflux kinetics via GLUT1 and the alterations observed with T295M is a harder task than mere simulation of inhibition of 2-DG influx at 37 °C and masking of this at low temperatures. However, using only one parameter alteration to accommodate the mutation at site 1 close to T295M, the four-site model simulates

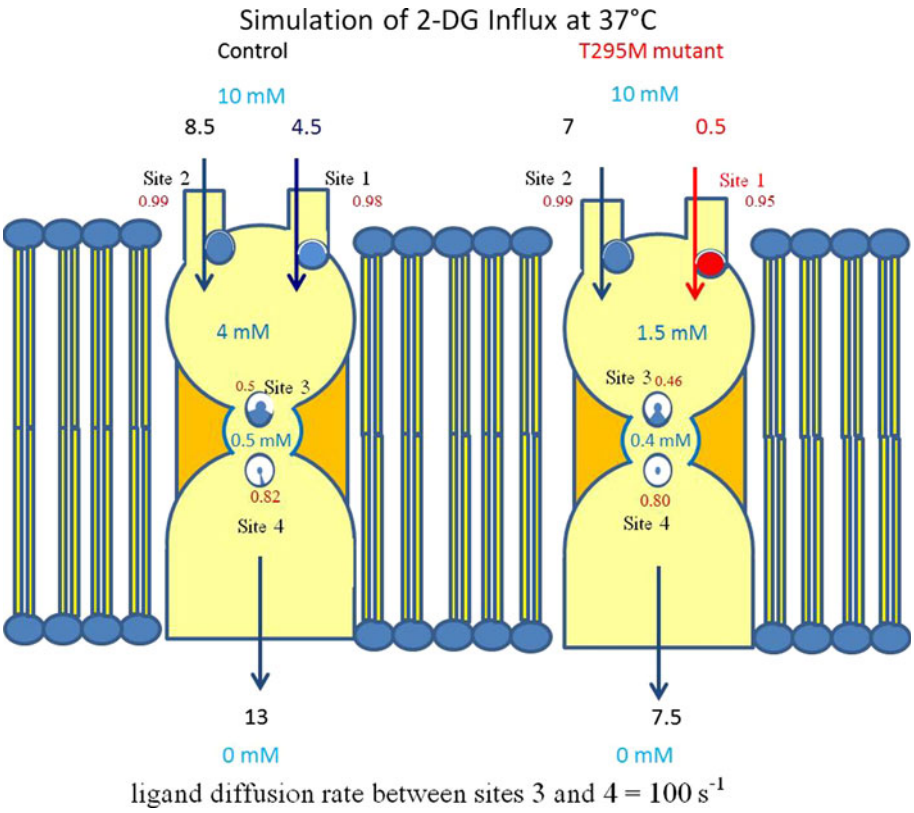

Fig. 6 Diagram showing comparison of net fluxes in control and T295M via sites 1–3 during influx of 2-DG at 37 °C. The diagram shows a snapshot of the fluxes when the external solution contains 10 mM and the internal solution contains 0 mM 2-DG. *Arrows* illustrate the fluxes via sites 1 and 2. Mutant flux via site 2 is reduced to 0.5 nmol min^{-1} from 8.5 nmol min^{-1} in control, whereas influx increases from 4 to 7 via site 1 because the retarded influx via site 1 reduces the vestibular 2-DG concentration from 4 mM (control) to 1.5 mM (T295M)

these complex kinetics and explains the alterations in terms of the local structural changes in the transporter.

As observed at 37 °C (Fujii et al. 2007; Wang et al. 2003, 2008; Wong et al. 2007), the simulated V_{max} of 3OMG influx is inhibited by 30 % when the T295M mutation retards access to site 1. Blocking sugar access to site 1 inhibits V_{max} net 3OMG efflux by ~70 %, as seen with the mutation T295M (Fujii et al. 2007; Wang et al. 2003, 2008; Wong et al. 2007). The lower V_{max} and higher K_m for 3OMG than 2-DG have been noted several times and are generally assumed to be caused by reduced affinity for the transporter resulting from *O*-methylation at C3 position (Cloherty et al. 1996; Miller 1971; Naftalin and Rist 1994). The main kinetic differences between 3OMG and 2-DG are simulated with the four-site model by reducing the diffusion rate of 3OMG through the narrow central channel between sites 3 and 4 by 50 % and raising the K_D of site 3 from 0.2 for 2-DG to 3 mM for 3OMG (Figs. 6, 7, 8, 9, 10, 11, 12). These alterations raise the apparent K_m for zero-trans of 3OMG net influx to 15 mM and reduce the V_{max} by ~50 % (Figs. 8, 10). These relatively large changes in the functional parameters are ascribable to the increased 3OMG accumulation in the external vestibule during zero-trans influx in comparison with 2-DG (Figs. 9c, 10d). When the external sugar concentration of 2-DG is 10 mM, its concentration in the external vestibule is 4 mM (Fig. 7). With external 3OMG at 10 mM, the vestibular 3OMG concentration is 8.8 mM (Fig. 10). The raised accumulation of 3OMG holds up net influx across the entire network and, in comparison with 2-DG, results in the relatively large changes in the functional parameters.

The parameters used to simulate the 30 % decrease in zero-trans influx V_{max} of 3OMG at 37 °C with the T295M mutation also simulate the very different effects of the mutation on 3OMG efflux at 37 °C (Fig. 10). Control 3OMG efflux has fivefold to tenfold higher V_{max} values than for influx, and similarly the K_m for efflux is fourfold to tenfold higher than for influx. Simulating the effects of the mutation T295M that blocks access to site 1 reduces the V_{max} for net efflux by threefold and decreases the K_m for net efflux from 40 to 7.5 mM, i.e., by approximately fivefold (Figs. 9, 11; Tables 1, 2, 3). The T295M mutation reduces efflux via site 1, resulting in higher 3OMG accumulation in the external vestibule than in control and leading to greater saturation of site 2 at lower external sugar concentrations and consequently to a reduced V_{max} of net efflux (Figs. 9, 11).

Discussion

Multiple Binding Sites Within the Ligand Trajectory Across the Transporter

A key attribute of the alternating-access transporter model is that transported ligands bind at a single centrally situated

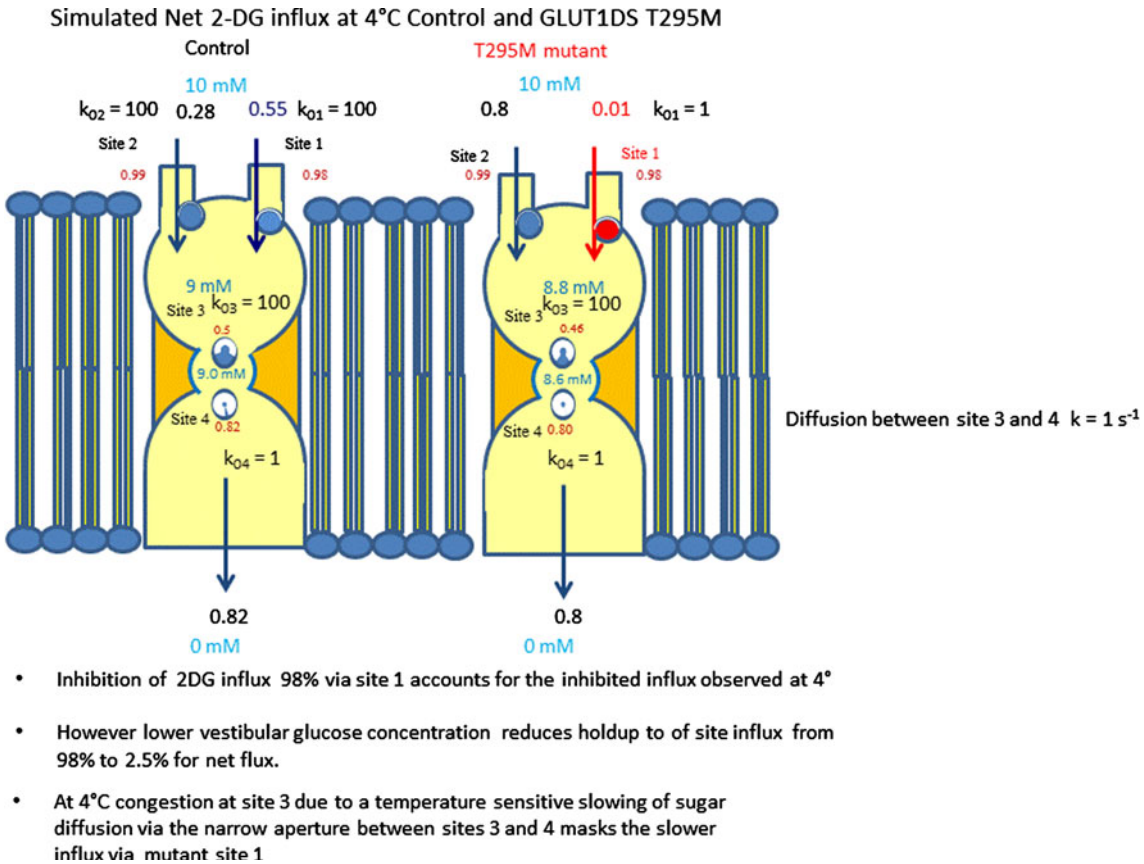

Fig. 7 Diagram showing simulated net 2-DG influx at 4 °C in control and T295M. The main difference between the simulations at 37 and 4 °C is that ligand diffusion is slowed at the lower temperature between sites 3 and 4. This is simulated here by reduction in the association dissociation rates at site 4 from 100 s^{-1} at 37 °C to 1 s^{-1} at 4 °C. The slower rate is to retard flux between sites 3 and 4 and results in sugar accumulation in the interspace between sites 3 and 4 with consequent accumulation of sugar in the external vestibule. This in turn retards influx from the external solutions via sites 1 and 2. However, because of the slower influx via the mutant site 1 2-DG accumulation in the external vestibule does not increase to the same extent as in control. With 10 mM in the external solution, the mutant vestibular concentration rises to 8.8 mM, whereas in the control it rises to 9.0 mM. This permits a higher influx via mutant site 2 than with control, which masks the 98 % reduction via mutant site 1 and consequently masks net flux across the transporter

occluding site (Jardetzky 1966). This implies that both the affinity and the selectivity toward transported ligand relate to the way in which the ligand interacts with that site. This view was first tested for GLUT1 (Barnett et al. 1973). With the advent of crystallographic structures of transporters, e.g., leucine transport via LeuT showing multiple binding sites (Singh et al. 2008), the concept that several coexistent ligand binding sites may be involved in the transmembrane transport process is becoming more accepted. A recent example illustrating multiple binding sites within a transporter has been uncovered in the *Aspergillus nidulans* uric acid-xanthine/H^+ symporter, using in silico docking and molecular mechanics combined with mutation studies (Kosti et al. 2012). Multiple binding sites are situated along a trajectory, extending from the cytosolic face to the centrally placed major binding site, whose wall is lined with polar side chains. The possibility of multiple or braided pathways through a transporter implies, as previously discussed (Cunningham et al. 2006), that ligand selectivity may be distributed over several sites. Multiple pathways with different selectivity toward ligands and water have been recently suggested as a possible explanation for the evident water permeability. Jiang et al. (2010) have shown in several GLUT1 mutants, S66F, F126K and T310I, in which glucose transport is impaired that both the organic arsenical, methylarsenate, and water permeabilities are increased and insensitive to cytochalasin B.

Sugar Binding Sites in the External Vestibule of GLUT1

The region adjacent to T295 in the linker between TMs 7 and 8 has been examined previously in several GLUT isoforms. In GLUT7, Ile-314 in the linker between TMs 7 and 8 is at an equivalent position to Val-290 in human GLUT1 (Manolescu et al. 2005). In wild-type GLUT7,

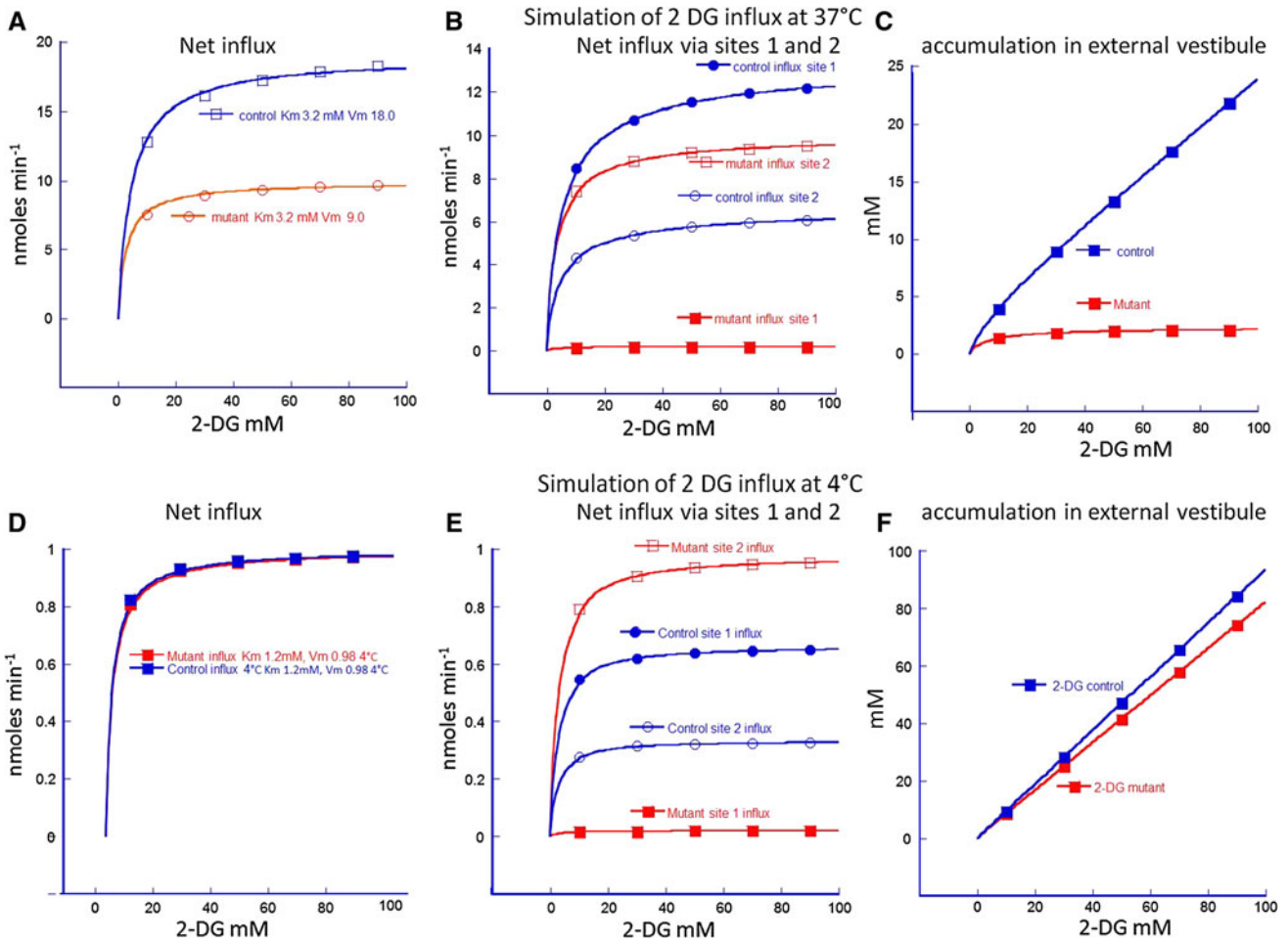

Fig. 8 Simulations of net influx of 2-DG at 4 and 37 °C in control and mutant T295M. **a** Simulations of 2-DG influx via control and T295M GLUT1 at 37 °C. The computed net influx is obtained by varying glucose over a range of 0–100 mM in the external solution. The flux parameters are obtained by least squares analysis of the simulated curves fitting to a Michaelis–Menten equation. **b** Fluxes via sites 1 (*open symbols*) and 2 (*filled symbols*) in control (*circles*) and mutant (*squares*). Negligible influx via mutant site 1 is observed. Influx via mutant site 2 exceeds influx via control site 2. **c** 2-DG accumulation in the external vestibule is much higher in control than with mutant as influx via mutant site 1 is lower. **d** The equivalent 2-DG influx as in **a** except the temperature is 4 °C. No difference between control and mutant net influx is observed. **e** 2-DG via sites 1 and 2. Influx via mutant site 1 is negligible. Influx via mutant site 2 exceeds that via control site 1 and site 2 so that there is no net difference. The major cause of the masking of the decreased influx via mutant site 1 at 4 °C is due to the raised sugar accumulation in the external vestibule as a result of the low rate of sugar flux between sites 3 and 4. Although sugar accumulation in the vestibule is much greater at 4 °C than at 37 °C (**c**), the mutant accumulation remains less than with control; hence, this permits the raised influx via mutant site 2

both glucose and fructose are transported with high affinity but the I314V mutation does not transport fructose, although glucose transport is unaffected (Manolescu et al. 2007). In GLUT2 the I322V mutation also loses the capacity to transport fructose but retains transport capacity for D-glucose. In GLUT5 the I296V mutant also loses fructose transport capacity without altered D-glucose transport (Manolescu et al. 2007).

The double QLS motif in TM7 of GLUT1 has been identified as a possible selectivity filter for glucose in preference to fructose (Seatter et al. 1998). This motif is within 6 Å of glucose docking cluster sites 1–3 within the external vestibule.

In the yeast *Saccharomyces cerevisiae* hexose transporter Hxt7, a high-affinity GLUT1 isoform, substitution of cysteine for asparagine at position 340, lying near the external end of TM7, enhances glucose affinity by 50 % (Kasahara et al. 2009). D-Glucose protected Cys-340 against reaction with pCMBS, indicating that it lies close to a sugar recognition site.

Additionally, three GLUT isoforms—LmGT1, LmGT2 and LmGT3—have been identified in the protozoan parasite *Leishmania mexicana*. LmGT2 has sixfold higher affinity for D-ribose than the transporter LmGT3. The high ribose specificity in LmGT2 is thought to be conferred by a pair of threonines in the external linkers, between TMs 3

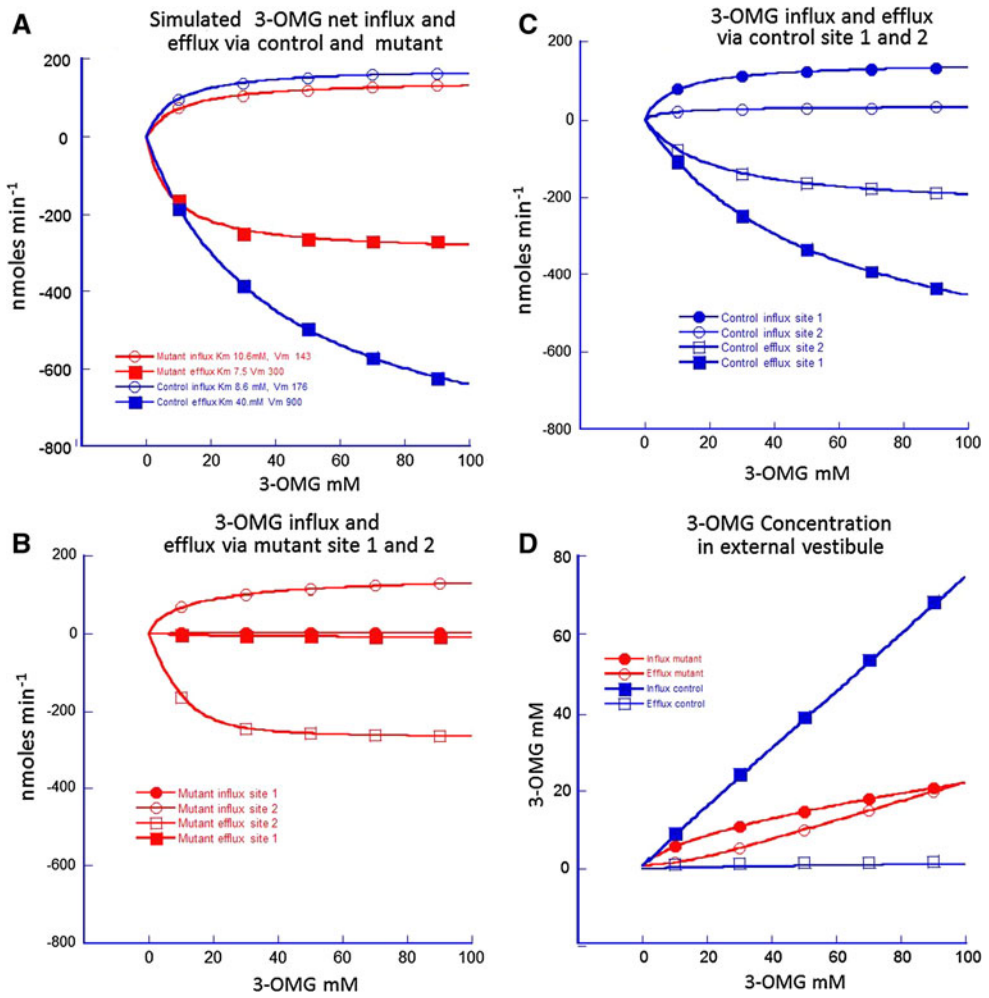

Fig. 9 Simulations of 3OMG zero-trans net influx and efflux via control and T295M mutant GLUT1 at 37 °C. **a** Simulations of 3OMG influx (positive fluxes) and effluxes (negative fluxes). The V_{max} of mutant influx is 143 nmol s^{-1} and K_m 10.6 mM compared with V_{max} influx of 176 nmol s^{-1} and $K_m = 8.6$ mM in control. The simulated net efflux parameters for control are V_{max} 900 nmol s^{-1} and $K_m = 40$ mM; the parameters for mutant efflux are V_{max} 300 nmol s^{-1}, K_m 7.5 mM. **b** Net influxes and effluxes via sites 1 and 2 in controls and **c** net influxes and effluxes via sites 1 and 2 in the mutant. Flux via site 1 predominates in control influx and efflux, whereas with the mutant fluxes via site 2 predominate and fluxes via site 1 are negligible. Efflux via site 2 in the mutant is limited by the relatively high accumulation of 3OMG in the external vestibule in the mutant (**d**, *open symbols*). This higher accumulation in the mutant vestibule is due to the blocked transport via site 1

and 4 at position 205 and between TMs 6 and 7 at position 365. This is corroborated by the observation that the double mutant T205A/T365A in LmG3 increased the K_m for ribose from 5.85 to 3.55 mM (Naula et al. 2010).

It has been suggested that the proximity between I296 and W89 in the outer vestibular rim of GLUT7 creates a hydrophobic narrowing, which could act as selectivity filter or gate for glucose and fructose prior to their binding at a centrally located inversion site (Manolescu et al. 2005). A similar view is suggested with regard to the threonine residues T205 and T 365 in *L. mexicana* LmGt2 (Naula et al. 2010).

The docking studies shown in Figs. 1, 2, 3, and 4 suggest that the effect of the M295 mutation or insertion mutation between positions 298 and 299 on sugar docking is localized within a radius of 7–10 Å, affecting mainly the affinities at the docking cluster 1, and includes approximately half of the exofacial surface of the transporter. This finding in accord with similar direct observations in yeast Hxt7 (Kasahara et al. 2009) indicates that T295 provides a hydrophilic surface that guides sugar to one of the optional entry branches in the outer vestibule (Fig. 2) and modifies this hydrophilic side chain to a hydrophobic methionyl residue, M295, or that, as in Fig. 3d, a methyl group can occlude this branch. The finding that other T295 missense mutants, e.g., G295 and A295, also affect the docking affinity at the adjacent site indicates that hydrophobic interactions are important influences on docking at this site.

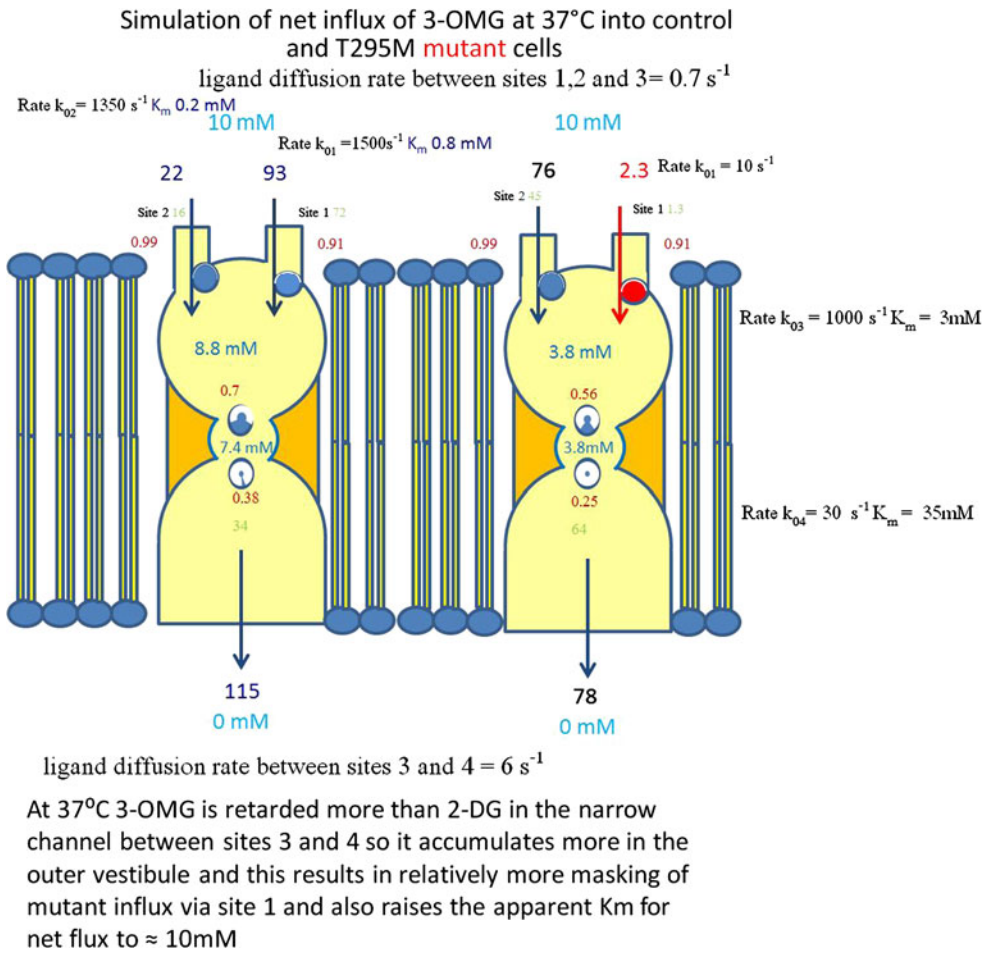

Fig. 10 Diagram showing 3OMG net influx in control and T295M mutant at 37 °C. The diagram shows a snapshot of the fluxes observed when the external solution has a 3OMG concentration of 10 mM and zero 3OMG in the internal solution. Comparison of the fluxes via site 1 show a 97.5 % reduction with the mutant, whereas influx via the mutant site 2 is increased by 3.45-fold. This is due to the reduced 3OMG accumulation into the mutant external vestibule and the intermediate space between sites 3 and 4 as a consequence of the reduced intake via site 1. The difference between the accumulation of 3OMG and 2-DG is mainly due to the higher relative resistance to 3OMG between sites 3 and 4

Thermosensitivity of GLUT1 Mutants

The temperature sensitivity of the glucose transport defects in T295M and the QQLS insertion between residues 298 and 299 mutants is an intriguing and previously unexamined phenomenon. The temperature sensitivity of channel and transporter mutants in general has been discussed in regard to TRP channels (Brauchi et al. 2004; Clapham and Miller 2011; Kim et al. 2013) and in relation to the *S. cerevisiae* monocarboxylate/H^+ symporter Jen1p (Soares-Silva et al. 2011). It has been suggested that temperature sensitivity involves large enthalpy or heat capacity changes requiring large conformational changes. The position of the cryosensitive mutant S271Q/E in the Jen1p symporter is consistent with this view (Soares-Silva et al. 2011). The transport defect is observed at 18 °C but not at 30 °C. S271 is thought to have a crucially important stabilizing role in facilitating helix packing in Jen1p symporter as it is hydrogen-bonded to the backbone of adjacent G267. However, the view that temperature sensitivity necessarily involves large conformational changes is challenged by the finding that a single temperature-specific residue, Y653C, is present in an extracellular pore loop of rat TRPV1. This indicates that only a small and localized conformational change is all that is required to trigger temperature sensitivity (Kim et al. 2013).

Positioning of GLUT1 T295M and 4-mer insertion mutants in an external vestibular loop is consistent with the view that these temperature-sensitive mutants are associated only with small conformational changes. Paradoxically, the temperature dependence for net glucose uptake is known to have a very high activation energy, around 150–200 kJ M^{-1}. Raising temperature between 17 and 37 °C increased the V_{max} for zero-trans entry by ~44-fold

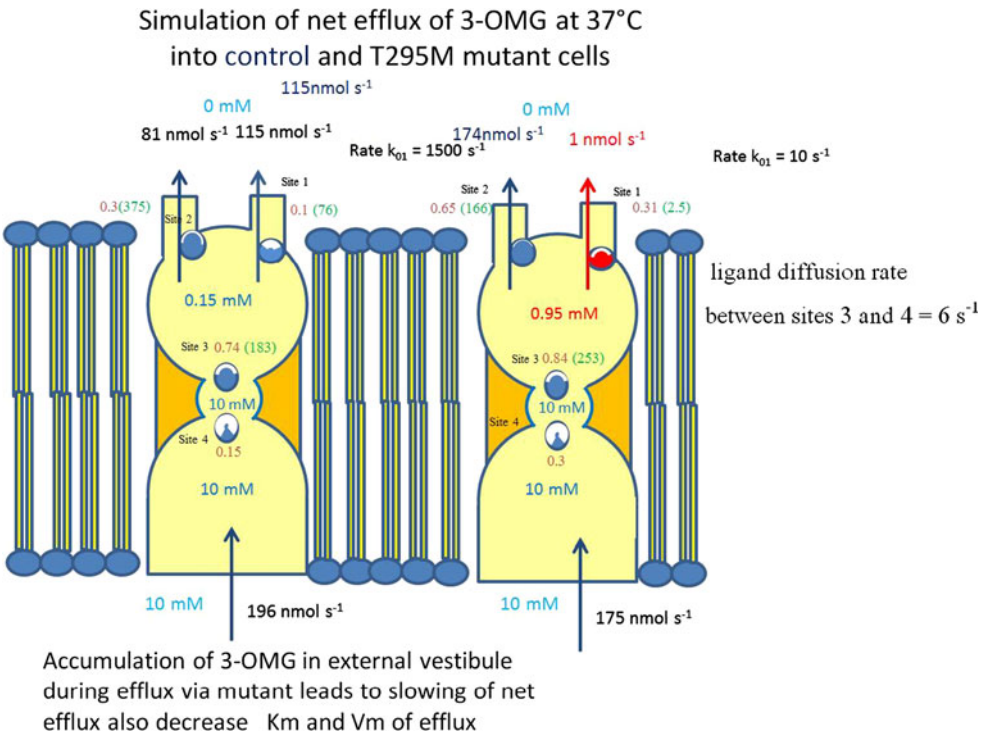

Fig. 11 Diagram showing 3OMG net efflux in control and T295M mutant at 37 °C. The diagram shows a similar snapshot of the fluxes in control and T295 with 3OMG concentration fixed at 10 mM in the internal solution and zero 3OMG in the external solution. The main difference between control and mutant fluxes is the retarded efflux via mutant site 1. This generates a higher 3OMG concentration in the mutant external vestibule 0.95 mM compared with 0.15 mM in control. This leads to a much higher saturation of mutant site 2 = 0.65 than in control = 0.3

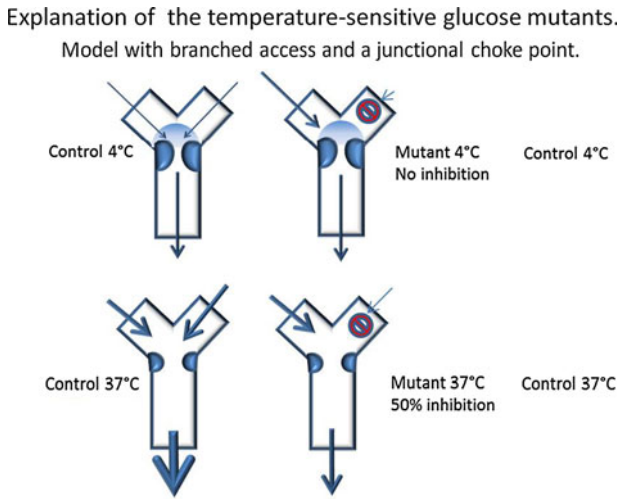

Fig. 12 Temperature-sensitive glucose mutants. This model requires only a small activation energy conformational change in the Y branch to make the transport defect. A large activation energy is required at the Y junction to permit rapid flow through to the common pathway

(Whitesell et al. 1989; Lowe and Walmsley 1986). It is apparent from this, because flow adjacent to T295 is only a single branch of a wider flow network, that the glucose uptake process in the vicinity of T295 is only one of possibly several other branches and more distal steps determining net glucose uptake from the external solution. The major enthalpic/entropic event is most likely to occur at the narrow central part of the molecule situated along with the high-affinity binding site. This central binding site is in a narrow channel surrounded by nine hydrophobic amino acids, six aromatic—F26, F229, Y292, F279, W388 and W412—and three aliphatic—I164, I168 and I287—as well as five polar amino acids—T30, Q161, Q282, Q283 and N288. It is likely that the activation energy of glucose traversal through this discrete narrow central region is large as it will inevitably lead to the making and breaking of many hydrogen bonds.

An explanation for the thermal sensitivity of glucose transport via the T295M mutant is that at low temperatures glucose flow is rate-limited by very high resistance to flow at the central part of the molecule. This results in glucose accumulation within the external vestibule, which slows net influx from the external solution to such an extent that the defective flow via the branch gated by M295 is obscured. However, at higher temperatures glucose flow through the central channel is much faster on account of its high activation energy, and consequently, the deficient glucose entry from the external solution at the defective gate at M295 is unmasked (Fig. 12).

This two-stage transit is a possible explanation for the existence of a thermosensitive mutant in the external linker where glucose transit has only a low activation energy.

The absence of significant affinity changes obtained with docking to the various alternative mutants at position 295 in GLUT1 (Fig. 3d) illustrates the difference between kinetic measurements of affinity which entail a combination of rates of diffusion from the external solution to the binding site and the binding affinity at the site, whereas the

Table 3 Comparison of flux parameters observed by Wang et al. (2003) with parameters derived from the simulations of 3OMG flux as shown in Fig. 10

Condition	Parameter	WT		T295M		WT/T295M	
		Obs	Model	Obs	Model	Obs	Model
Influx	$K_{m\ out}$ (mM)	9.6	8.5	14.3	10.6	0.7	0.75
	$V_{max\ out\ (pmol/min/oocyte)}$	747	176	590	143	1.3	1.2
	V_{max}/K_m	77.8	20.7	41.3	13.4	1.9	1.5
Efflux	K_{min}	91.0	40.00	8.8	7.5	10.3	5.3
	$V_{max\ in\ (pmol/min/oocyte)}$	7,443	900	1,216	300	6.1	3.0
	$V_{max\ in}/K_{m\ in}$	82.0	22.5	138	40	0.6	0.56
Asymmetry	$K_{max\ in}/K_{m\ out}$	9.5	4.7	0.6	0.83	16	29
	$V_{max\ in}/V_{max\ out}$	10.0	5.1	2.1	2.1	4.8	8.6
	Haldane ratio	0.95	0.92	0.29	0.33		
	$V_{max\ out}/K_{m\ out}/(V_{maxin}/K_{min})$					3.3	2.8

steady-state affinities obtained by equilibrium dialysis or derived from in silico docking studies are based more nearly on the intrinsic binding affinity of the groups at the binding site. The docking affinities are much higher at the centrally located sites than those obtained by kinetic measurements (Figs. 1, 3d; Tables 1, 2) and apparently are independent of any of the mutations that we have monitored.

T295M and Altered Glucose Flux Asymmetry

Simulation of the parallel entry paths via sites 1 and 2 converging on a central site 3 and continuing to a fourth inside site reflects the main observed features of the changes in asymmetric 3OMG influx and efflux kinetics. Simulation of the T295M mutation mirrors the thermal sensitivity observed with the T295M and the 4-mer QQLS insertion mutants. The flux asymmetry demonstrated in the behavior of 3OMG transport via the GLUT1 transporter and illustrated in Figs. 9, 10, 11, and 12 shows that interference at one node in the network, e.g., at site 1, can cause asymmetric inhibition of net influx and net efflux. As seen in Figs. 5, 6 and 12 GLUT1DS mutations situated in more central regions of the transporter will affect all the converging influx or diverging efflux streams. A defect in this central region is unlikely to lead to transporter deficiencies that have temperature sensitivity or that greatly alter the flux asymmetry but instead will simply cause a symmetrical inhibition of glucose influx and efflux.

The principle of detailed balance requires that the product of clockwise rate constants around any closed cyclic network, as envisaged by the single-site alternating-access transport model at equilibrium, should equal the product of anticlockwise rates. To conform to detailed balancing, the Haldane ratio should equal unity (Lieb and Stein 1974; Lowe and Walmsley 1986; Cloherty et al. 1996; Naftalin 2008, 2010). Reversal of the asymmetric affinities of 3OMG with the GLUT1DS T295M mutation has important mechanistic implications as this subverts the conventional view that glucose transport conforms to an asymmetric alternating carrier model in which ligand selectivity is localized at a central site, such as the QLS motif in TM7 (Seatter et al. 1998).

Interpreting the 3OMG flux kinetics via the T295M GLUT1DS mutant in terms of the conventional alternating-access model requires that the single T295M mutation affects the sugar affinity more strongly on the inside than the outside transporter face. Mutations fixed in the external linker between TM7 and -8 have no possibility of participation in sugar binding to the export site yet have large inhibitory effects on efflux K_m and V_{max}. Since the mutation reduces the maximal rate of sugar exit to a greater extent than the maximal entry rate, the model predicts that the ratio of inward to outward flux rates of unliganded carrier is altered by the mutation from 9.5 to 0.6, implying that the mutation decreases vacant carrier influx by 15- to 16-fold. These kinetics are irreconcilable with the single-site alternate-access model but, as has been demonstrated here, are readily accommodated with transport via a network of several fixed sites on opposing sides of the transporter (Naftalin 2008, 2010; Carruthers et al. 2009; Leitch and Carruthers 2009).

This finding is therefore inconsistent with current perceptions of the mechanism of alternating-access transport.

Implications of this Study for Practical Diagnosis of GLUT1DS

It is important that the clinical finding of hypoglycorrhachia be corroborated with a reliable functional test of glucose transporter deficiency. Sugar efflux measurements are technically more demanding than influx measurements,

so it is desirable that a more reliable method of monitoring sugar influx is found. The docking data and the simulations here suggest that either radioactively labeled 2-DG or D-glucose at higher temperature, around 24 °C, should be employed instead of 3OMG to assay influx as influx of these sugars is evidently less affected. If higher sugar concentrations, between 10 and 50 mM, are used, equilibration will take between 2 and 3 min and will more likely show a transport defect than with 3OMG, which appears to be more retarded in the narrow central channel than either 2-DG or glucose.

Acknowledgments The authors thank Drs. Louis J. De Felice, VCU School of Medicine, Richmond, VA, USA; Darryl C. De Vivo, New York Presbyterian Hospital, Columbia University, New York, NY, USA; George Diallinas, National and Kapodistrian Faculty of Biology, University of Athens, Greece; Tasuya Fujii Shiga Medical Center for Children, Moriyama, Japan; Joerg Klepper, Childrens' Hospital, Aschaffenburg, Germany; and Andrea Parmegianni, Theoretical Physics, University of Montpelier, France, for their invaluable guidance and discussions during the course of this work.

References

Barnett JE, Holman GD, Munday KA (1973) Structural requirements for binding to the sugar-transport system of the human erythrocyte. Biochem J 131:211–221

Brahm J (1983) The kinetics of glucose transport in human erythrocytes. J Physiol 339:339–354

Brauchi S, Orio P, Latorre R (2004) Clues to understanding cold sensation: thermodynamics and electrophysiological analysis of the cold receptor TRPM8. Proc Natl Acad Sci USA 101:15494–15499

Brockmann K (2009) The expanding phenotype of GLUT1-deficiency syndrome. Brain Dev 31:545–552

Butterfoss GL, Hermans J (2003) Boltzmann-type distribution of side-chain conformation. Protein Sci 203:2719–2731

Carruthers A, DeZutter J, Ganguly A, Devaskar SU (2009) Will the original glucose transporter isoform please stand up! Am J Physiol Endocrinol Metab 297:E836–E848

Chou T, Mallick K, Zia RKP (2011) Non-equilibrium statistical mechanics: from a paradigmatic model to biological transport. Rep Prog Phys 74:116601

Clapham DE, Miller C (2011) A thermodynamic framework for understanding temperature sensing by transient receptor potential (TRP) channels. Proc Natl Acad Sci USA 108:19492–19497

Cloherty EK, Heard KS, Carruthers A (1996) Human erythrocyte sugar transport is incompatible with available carrier models. Biochemistry 35:10411–10421

Cunningham P, Afzal-Ahmed I, Naftalin RJ (2006) Docking studies show that D-glucose and quercetin slide through the transporter GLUT1. J Biol Chem 281:5797–5803

Fujii T, Ho Y–Y, Wang D, De Vivo DC, Miyajima T, Wong H-Y, Tsang P-T, Shirasaka Y, Kudo T, Ito M (2007) Three Japanese patients with glucose transporter type 1 deficiency syndrome. Brain Dev 29:92–97

Fujii T, Morimoto M, Yoshioka H, Ho Y–Y, Law PPY, Wang D, Vivo DCD (2011) T295 M-associated Glut1 deficiency syndrome with normal erythrocyte 3OMG uptake. Brain Dev 33:316–320

Fung EL-W, Yuan Y, Hui J, Ho J (2011) First report of GLUT1 deficiency syndrome in Chinese patients with novel and hot spot mutations in *SLC2A1* gene. Brain Dev 33:170–173

Jardetzky O (1966) Simple allosteric model for membrane pumps. Nature 211:969–970

Jiang X, McDermott JR, Ajees AA, Rosen BP, Liu Z (2010) Trivalent arsenicals and glucose use different translocation pathways in mammalian GLUT1. Metallomics 2:211–219

Kasahara T, Maeda M, Boles E, Kasahara M (2009) Identification of a key residue determining substrate affinity in the human glucose transporter GLUT1. Biochim Biophys Acta 1788:1051–1055

Kim SE, Patapoutian A, Grandl J (2013) Single residues in the outer pore of TRPV1 and TRPV3 have temperature-dependent conformations. PLoS ONE 8:3

Klepper J (2012) GLUT1 deficiency syndrome in clinical practice. Epilepsy Res 100:272–277

Kosti V, Lambrinidis G, Myrianthopoulos V, Diallinas G, Mikros E (2012) Identification of the substrate recognition and transport pathway in a eukaryotic member of the nucleobase-ascorbate transporter (NAT) family. PLoS ONE 7:7

Leitch JM, Carruthers A (2009) Alpha- and beta-monosaccharide transport in human erythrocytes 8. Am J Physiol Cell Physiol 296:C151–C161

Lieb WR, Stein WD (1974) Testing and characterizing the simple carrier 2. Biochim Biophys Acta 373:178–196

Liu X, O'Donnell N, Landstrom A, Skach WR, Dawson DC (2012) Thermal instability of ΔF508 cystic fibrosis transmembrane conductance regulator (CFTR) channel function: protection by single suppressor mutations and inhibiting channel activity. Biochemistry 51:5113–5124

Lowe AG, Walmsley R (1986) The kinetics of glucose transport in human red blood cells. Biochim Biophys Acta 857:146–154

Manolescu A, Salas-Burgos AM, Fischbarg J, Cheeseman CI (2005) Identification of a hydrophobic residue as a key determinant of fructose transport by the facilitative hexose transporter SLC2A7 (GLUT7). J Biol Chem 280:42978–42983

Manolescu AR, Augustin R, Moley K, Cheeseman C (2007) A highly conserved hydrophobic motif in the exofacial vestibule of fructose transporting SLC2A proteins acts as a critical determinant of their substrate selectivity. Mol Membr Biol 24:455–463

Miller DM (1971) The kinetics of selective biological transport. V. Further data on the erythrocyte-monosaccharide transport system. Biophys J 11:915–923

Mueckler M, Caruso C, Baldwin SA, Panico M, Blench I, Morris HR, Allard WJ, Lienhard GE, Lodish HF (1985) Sequence and structure of a human glucose transporter. Science 229:941–945

Naftalin R (2008) Alternating carrier models of asymmetric glucose transport violate the energy conservation laws. Biophys J 95:4300–4314

Naftalin RJ (2010) Reassessment of models of facilitated transport and cotransport. J Membr Biol 234:75–112

Naftalin RJ, Rist RJ (1994) Re-examination of hexose exchanges using rat erythrocytes: evidence inconsistent with a one-site sequential exchange model, but consistent with a two-site simultaneous exchange model. Biochim Biophys Acta 1191:65–78

Naula CM, Logan FM, Wong PE, Barrett MP, Burchmore RJ (2010) Definition of residues that confer substrate specificity in a sugar. J Biol Chem 285:29721–29728

Pantazopoulou A, Diallinas G (2006) The first transmembrane segment (TMS1) of UapA contains determinants necessary for expression in the plasma membrane and purine transport. Mol Membr Biol 23:337–348

Parmeggiani A, Franosch T, Frey E (2004) Totally asymmetric simple exclusion process with Langmuir kinetics. Phys Rev E 70:1–20

Rotstein M, Engelstad K, Yang H, Wang D, Levy B, Chung WK, De Vivo DC (2010) Glut1 deficiency: inheritance pattern determined by haploinsufficiency. Ann Neurol 68:955–958

Salas-Burgos A, Iserovich P, Zuniga F, Vera JC, Fischbarg J (2004) Predicting the three-dimensional structure of the human

facilitative glucose transporter glut1 by a novel evolutionary homology strategy: insights on the molecular mechanism of substrate migration, and binding sites for glucose and inhibitory molecules. Biophys J 87:2990–2999

Seatter MJ, De la Rue SA, Porter LM, Gould GW (1998) QLS motif in transmembrane helix VII of the glucose transporter family interacts with the C-1 position of D-glucose and is involved in substrate selection at the exofacial binding site. Biochemistry 37:1322–1326

Seeliger D, de Groot BL (2010) Ligand docking and binding site analysis with PyMOL and autodock/vina. J Comput Aided Mol Des 24:417–422

Seeliger D, Buelens FP, Goette M, de Groot BL, Grubmüller H (2011) Towards computational specificity screening of DNA-binding proteins. Nucleic Acids Res 39:8281–8290

Sen AK, Widdas WF (1962) Determination of the temperature and pH dependence of glucose transfer across the human erythrocyte measured by glucose exit. J Physiol 160:393–403

Singh SK, Piscitelli CL, Yamashita A, Gouaux E (2008) A competitive inhibitor traps LeuT in an open-to-out conformation. Science 322:1655–1661

Soares-Silva I, Sá-Pessoa J, Myrianthopoulos V, Mikros E, Casal M, Diallinas G (2011) A substrate translocation trajectory in a cytoplasm-facing topological model of the monocarboxylate/H^+ symporter Jen1p. Mol Microbiol 81(3):805–817

Sun L, Zeng X, Yan C, Sun X, Gong X, Rao Y, Yan N (2012) Crystal structure of a bacterial homologue of glucose transporters GLUT1-4. Nature 490:361–366

Trott O, Olson AJ (2010) Software news and update autodock vina: improving the speed and accuracy of docking with a new scoring function, efficient optimization, and multithreading. J Comput Chem 31:455–461

Wang D, Pascual JM, Iserovich P, Yang H, Ma L, Kuang K, Zuniga FA, Sun RP, Swaroop KM, Fischbarg J, De Vivo DC (2003) Functional studies of threonine 310 mutations in Glut1: T310I is pathogenic, causing Glut1 deficiency. J Biol Chem 278:49015–49021

Wang D, Yang H, Shi L, Ma L, Fujii T, Engelstad K, Pascual JM, De Vivo DC (2008) Functional studies of the T295 M mutation causing glut deficiency: glucose efflux preferentially affected by T295 M. Pediatr Res 64:538–543

Whitesell RR, Regen DM, Beth AH, Pelletier DK, Abumrad NA (1989) Activation energy of the slowest step in the glucose carrier cycle: break at 23 °C and correlation with membrane lipid fluidity. Biochemistry 28:5618–5625

Wong HY, Law PY, Ho YY (2007) Disease-associated Glut1 single amino acid substitute mutations S66F, R126C, and T295 M constitute Glut1-deficiency states in vitro. Construction 90: 193–198